Article

Immunity

Inhibition of transcription factor NFAT activity in activated platelets enhances their aggregation and exacerbates gram-negative bacterial septicemia

Graphical abstract

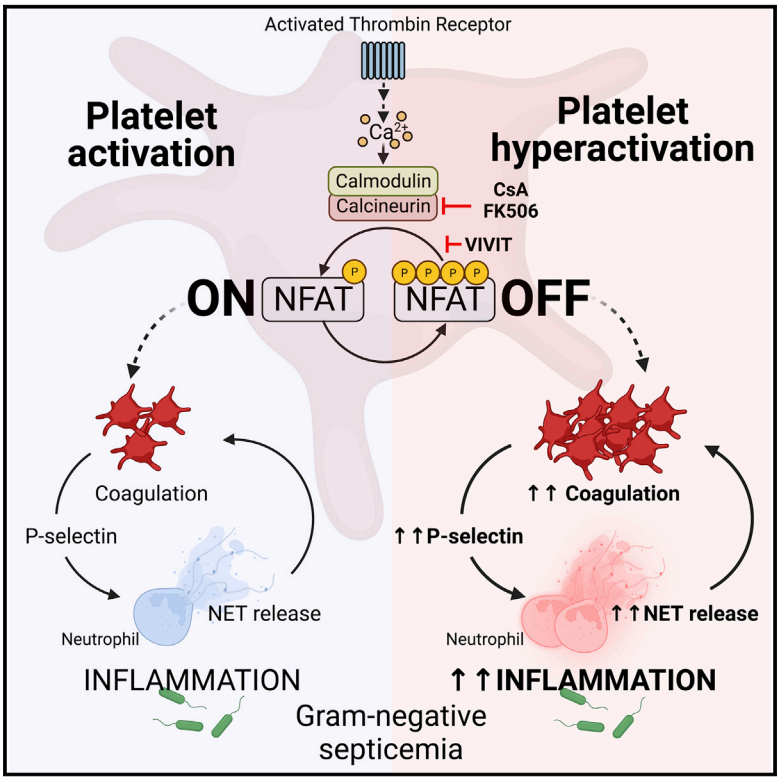

Highlights

- Thrombin receptor signaling activates NFAT in human and mouse platelets
- Inhibition of NFAT in platelets promotes aggregation and neutrophil interactions
- NFAT inhibition potentiates coagulation in patients with hypoactive platelets
- NFAT blockade in platelets boosts NETosis and inflammation in bacterial septicemia

Authors

Valentina Poli, Marco Di Gioia, Martha Sola-Visner, Francesca Granucci, Andrew L. Frelinger III, Alan D. Michelson, Ivan Zanoni

Correspondence

ivan.zanoni@childrens.harvard.edu

In brief

The pathways controlling platelet-neutrophils interactions remain unclear. Poli et al. demonstrate that the transcription factor NFAT regulates the hemostatic and inflammatory activities of platelets. NFAT inhibition in activated platelets increases dense granule release, platelet aggregation, and interactions with neutrophils. NFAT inhibition in platelets *in vivo* initiates a detrimental feedback loop that enhances disseminated coagulation and NETosis and aggravates bacterial septicemia.

Poli et al., 2022, Immunity *55*, 224–236
February 8, 2022
https://doi.org/10.1016/j.immuni.2021.12.002

CellPress

CellPress

Immunity

Article

Inhibition of transcription factor NFAT activity in activated platelets enhances their aggregation and exacerbates gram-negative bacterial septicemia

Valentina Poli,[1] Marco Di Gioia,[1] Martha Sola-Visner,[2] Francesca Granucci,[3] Andrew L. Frelinger III,[4] Alan D. Michelson,[4] and Ivan Zanoni[1,5,6,7,*]

[1]Harvard Medical School, Boston Children's Hospital, Division of Immunology, Boston, MA, USA
[2]Harvard Medical School, Boston Children's Hospital, Division of Newborn Medicine, Boston, MA, USA
[3]Department of Biotechnology and Biosciences, University of Milano—Bicocca, INGM-National Institute of Molecular Genetics "Romeo ed Enrica Invernizzi", Milan, Italy
[4]Center for Platelet Research Studies, Dana-Farber/Boston Children's Cancer and Blood Disorders Center, Harvard Medical School, Boston, MA, USA
[5]Harvard Medical School, Boston Children's Hospital, Division of Gastroenterology, Boston, MA, USA
[6]Lead contact
[7]Twitter: @Lo_Zanzi
*Correspondence: ivan.zanoni@childrens.harvard.edu
https://doi.org/10.1016/j.immuni.2021.12.002

SUMMARY

During gram-negative septicemia, interactions between platelets and neutrophils initiate a detrimental feedback loop that sustains neutrophil extracellular trap (NET) induction, disseminated intravascular coagulation, and inflammation. Understanding intracellular pathways that control platelet-neutrophil interactions is essential for identifying new therapeutic targets. Here, we found that thrombin signaling induced activation of the transcription factor NFAT in platelets. Using genetic and pharmacologic approaches, as well as iNFAT-uation, a newly developed mouse model in which NFAT activation can be abrogated in a cell-specific manner, we demonstrated that NFAT inhibition in activated murine and human platelets enhanced their activation and aggregation, as well as their interactions with neutrophils and NET induction. During gram-negative septicemia, NFAT inhibition in platelets promoted disease severity by increasing disseminated coagulation and NETosis. NFAT inhibition also partially restored coagulation *ex vivo* in patients with hypoactive platelets. Our results define non-transcriptional roles for NFAT that could be harnessed to address pressing clinical needs.

INTRODUCTION

Sepsis is caused by microorganism-disseminated infection, with gram-negative bacteria-driven septicemia accounting for ~60% of all cases (Cohen, 2002). Treatment for this condition includes administration of antibiotics and fluids and costs 20 billion dollars per year (Williams, 2012). To date, all immunomodulatory therapies developed to treat sepsis or gram-negative septicemia have failed during clinical trials, highlighting an urgent need to unravel the pathophysiology of this syndrome, with the goal of developing new effective drugs.

Sepsis is characterized by a host response that includes release of cytokines by innate immune cells to combat the infection and is often associated with thrombosis (Jackson et al., 2019). Disseminated intravascular coagulation is a hallmark of severe sepsis and is a major cause of mortality. However, current anticoagulant pharmacological treatments are not very effective in treating sepsis, especially due to bleeding complications (Jackson et al., 2019). Thus, a better understanding of the cellular and molecular pathways that lead to disseminated coagulation in sepsis is imperative for designing new therapeutic interventions. Caspase-11 and gasdermin-D activated via high-mobility group box 1 (HMGB-1)-dependent relocation of lipopolysaccharide (LPS) in the cytoplasm of macrophages participate in sepsis and disseminated intravascular coagulation (Deng et al., 2018; Hagar et al., 2013; Kayagaki et al., 2015, 2013; Tang et al., 2021; Wu et al., 2019; Yang et al., 2019). Neutrophils also play key roles during sepsis. Neutrophil extracellular traps (NETs) are major drivers of disseminated coagulation during gram-negative bacterial septicemia (Jimenez-Alcazar et al., 2017; Xu et al., 2009), and their formation is tightly regulated by extrinsic and intrinsic programs (Adrover et al., 2020; Brinkmann et al., 2004; Poli et al., 2021; Saitoh et al., 2012). Recent studies demonstrate that interactions between platelets and neutrophils are critical for driving the formation of NETs and in sustaining disseminated coagulation (Clark et al., 2007; McDonald et al., 2012, 2017). In this context, platelets are activated not only by the coagulation cascade (e.g., thrombin) but also by direct

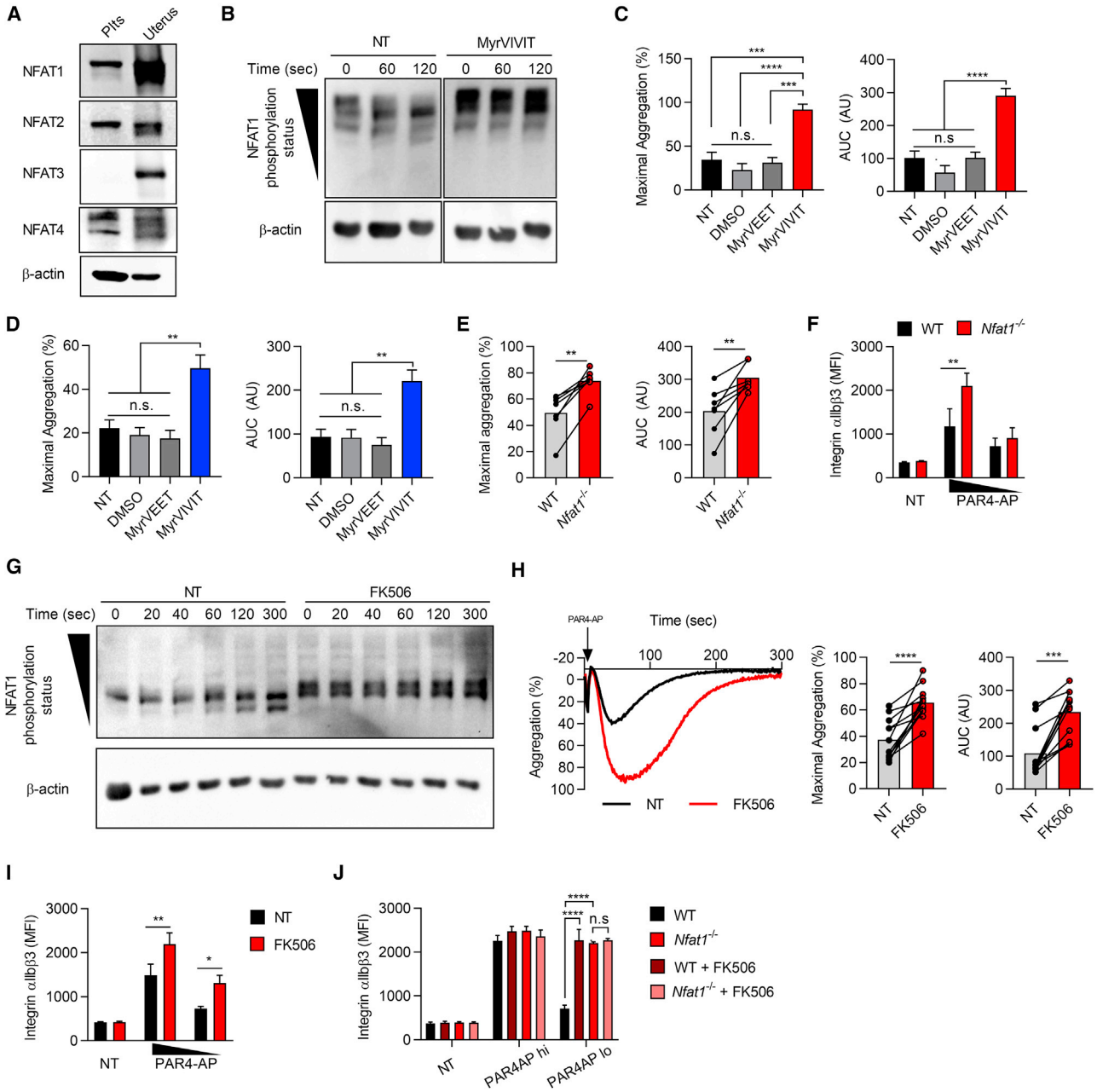

Figure 1. NFAT is activated upon stimulation of the thrombin receptor and modulates platelet aggregation

(A) Western blot analysis of NFAT1, NFAT2, NFAT3, and NFAT4 was performed on lysates from murine platelets or the uterine tissue. One experiment representative of three experiments.

(B) Phos-tag western blot analysis of mouse platelets pretreated, or not, with myristoylated VIVIT (MyrVIVIT) (10 μM) for 30 min and then stimulated with PAR4-AP (100 μM) for the indicated time points. One experiment representative of three experiments.

(C) Murine platelets were pretreated, or not, with vehicle (DMSO), the myristoylated control peptide (MyrVEET), or MyrVIVIT (10 μM) for 10 min and then activated with PAR4-AP (75 μM). Aggregation was monitored for 5 min. Histograms represent the percentage of maximal aggregation and area under curve (AUC). Data represent mean ± SEM. n ≥ 3 independent experiments.

(D) Human platelets were treated as in (C) and stimulated with TRAP (5 μM). Histograms represent the percentage of the maximal aggregation and AUC. Data represent mean ± SEM. n ≥ 3 independent experiments.

(E) Platelet-rich plasma (PRP) from WT or *Nfat1*$^{-/-}$ mice was stimulated with PAR4-AP (150 μM). Histograms represent the percentage of maximal aggregation and AUC. Each dot represents an independent test and lines highlight measurements performed concomitantly.

(F) PRP from WT or *Nfat1*$^{-/-}$ mice was stimulated with PAR4-AP (150 and 100 μM). Integrin αIIbβ3 activation was analyzed by cytofluorimetry. Bars represent the mean fluorescence intensity (MFI). Data represent mean ± SEM. n ≥ 3 independent experiments.

(G) Representative phos-tag western blot analysis of murine platelets pretreated, or not, with 1 μM FK506 for 1 h and then stimulated with PAR4-AP (100 μM) for the indicated time.

(legend continued on next page)

encounter with the invading pathogen and/or by direct interaction with neutrophils. In particular, activated platelets can recruit neutrophils and induce the release of NETs (Carestia et al., 2016; Liu et al., 2016; Sreeramkumar et al., 2014). Simultaneously, NET components further contribute to platelet activation and result in a detrimental feedback loop that leads to disseminated intravascular coagulation, poor tissue organ oxygenation, and organ failure (Elaskalani et al., 2018; Rossaint et al., 2016).

Multiple intersecting pathways lead to platelet activation (Rivera et al., 2009). Notably, although platelets do not have a nucleus, they bear transcription factors in their cytoplasm (Lannan et al., 2015). These transcription factors were long believed to be merely remnants of megakaryocytes. Nevertheless, scattered reports suggest that transcription factors that regulate immune cell functions—such as NF-κB or PPARϒ—also regulate the hemostatic activity of platelets (Akbiyik et al., 2004; Malaver et al., 2009). Despite these findings, the possibility that other transcription factors involved in the regulation of the immune response also regulate hemostatic or immune functions of platelets has been largely overlooked.

Here, we tested the hypothesis that another immune regulatory transcription factor, nuclear factor of activated T cells (NFAT), also modulates platelet function. By using a multi-pronged approach, we demonstrate that targeting the non-transcriptional activity of the NFAT in platelets holds promise for the development of innovative therapeutic approaches for life-threatening platelet dysfunctions and offers an interventional strategy to modulate disseminated intravascular coagulation and NETosis during gram-negative bacterial septicemia. Overall, our data demonstrate that physiological activation of NFAT in platelets functions as a fundamental checkpoint that controls platelet aggregation, interaction between platelets and neutrophils, induction of NETs during sepsis, and thereby modulates inflammation.

RESULTS

NFAT is activated upon stimulation of the thrombin receptor and modulates platelet aggregation

We first evaluated the presence of calcium-activated NFAT family members, and the p65 subunit of NF-κB as a control, in mouse platelets and found that, as with other immune cells, murine platelets express NFAT1, NFAT2, and NFAT4 but not NFAT3 (Figures 1A and S1A). Protein lysates from uterine tissue, which expresses all four NFAT members (Lizio et al., 2019), were used as controls (Figure 1A). Since our platelet preparation contained a small fraction of leukocytes (Figure S1B), we excluded that NFAT can be detected in a similar number of leukocytes (Figure S1A). Human platelets and murine platelets presented similar NFAT expression patterns (Figure S1C).

NFAT activation in immune cells is driven by activating phospholipase C (PLC) and by calcium influx, which then activates calcineurin and dephosphorylates NFAT (Zanoni and Granucci, 2012). Thus, we tested whether stimulation of the protease-activated receptor (PAR) in platelets with use of the PAR4-AP synthetic peptide, which leads to PLC activation and calcium influx, also dephosphorylates NFAT. We focused on NFAT1—a member of the NFAT family highly expressed in murine and human platelets (Figure S1C)—and found that activation of platelets led to a time-dependent dephosphorylation of NFAT1 (Figure 1B). Given that NFAT in immune cells is dephosphorylated by calcineurin, we used the permeable peptide VIVIT to specifically inhibit the interaction between calcineurin and NFAT (Aramburu et al., 1999) and observed an accumulation of phosphorylated NFAT1 in activated platelets treated with the VIVIT peptide (Figure 1B). This result demonstrates that NFAT can be dephosphorylated in anucleated cells, such as platelets.

Given that PAR activation in platelets leads to their efficient aggregation (Li et al., 2010), we tested if and how NFAT activation impacts platelet aggregation. Washed murine platelets showed a hyperaggregated phenotype in response to PAR4-AP when exposed to VIVIT but not to the control VEET peptide or to vehicle (Figure 1C). Similar results were also obtained with human platelets (Figure 1D), demonstrating that the interaction between NFAT and calcineurin affects the aggregation capacity of platelets across species.

The capacity of NFAT to regulate platelet aggregation upon PAR stimulation was confirmed in NFAT1-deficient mice. Wild-type (WT) and *Nfat1*$^{-/-}$ mice present a similar number of platelets in their blood (Figure S1D), excluding major defects in platelet formation due to NFAT1-deficiency. Platelet-rich plasma (PRP) from Nfat1$^{-/-}$ mice aggregated more efficiently compared with PRP derived from WT mice in response to PAR4-AP administration but not in homeostatic conditions (Figures 1E and S1E). A similar response was seen with use of washed platelets, demonstrating that plasma components are not responsible for the hyperactivated phenotype of *Nfat1*$^{-/-}$ platelets (Figure S1F). These data reveal that absence of NFAT1 in platelets is sufficient to induce hyperaggregation of PAR-stimulated cells.

Platelet aggregation depends on activation of the integrin αIIbβ3 (Bennett, 2005). Therefore, we examined whether the increased aggregation observed when NFAT is inhibited or deleted was also associated with increased activation of αIIbβ3. We found that genetic absence of NFAT1 resulted in a significant upregulation of αIIbβ3 integrin activation compared with that in WT platelets (Figure 1F), and this enhancement led to a more efficient spreading of platelets on fibrinogen (Figure S1G). In contrast, WT and NFAT1-deficient platelets showed no changes in the activation of p38 and Src (Figure S1H), two kinases previously suggested to control platelet aggregation downstream of calcineurin (Khatlani et al., 2014).

Inhibition of NFAT activation via calcineurin inhibitors, such as FK506 (also known as tacrolimus) and cyclosporin A (CsA), is a broadly utilized immunosuppressive treatment in patients with transplants (Azzi et al., 2013), and altered platelet functionality

(H) Murine PRP was treated as in (G). Aggregation curves and histograms of maximal aggregation and AUC are shown. Each dot represents an independent test.
(I) PRP was pretreated as in (G) and then stimulated with different concentration of PAR4-AP (150 and 100 μM). Integrin αIIbβ3 activation was analyzed by cytofluorimetry. Bars represent the MFI. Data represent mean ± SEM. n ≥ 3 independent experiments.
(J) PRP from WT or *Nfat1*$^{-/-}$ mice was pretreated as in (G), and integrin αIIbβ3 activation was analyzed by cytofluorimetry. Data represent mean ± SEM. n ≥ 3 independent experiments. One-way ANOVA (C and D), unpaired two-tailed t test (E and H), or two-way ANOVA (F, I, and J) were used for statistics. n.s., not significant ($p > 0.05$), **$p < 0.01$, ***$p < 0.001$, and ****$p < 0.0001$. See also Figure S1.

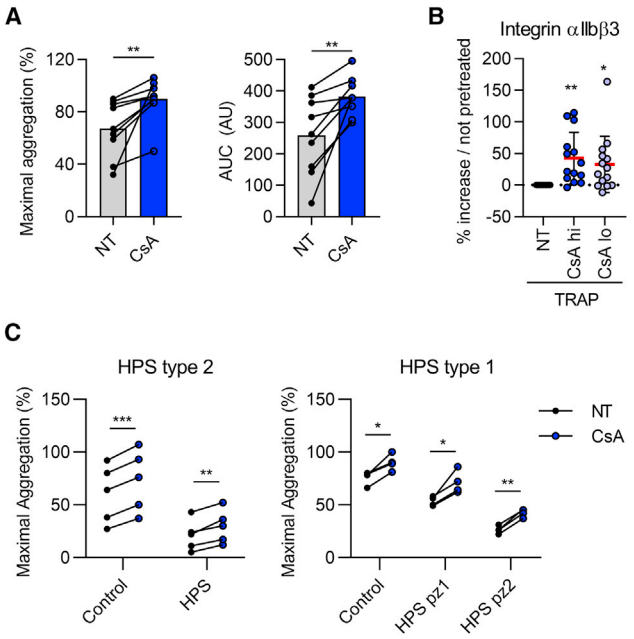

Figure 2. NFAT inhibition potentiates the aggregation of human hypoactive platelets

(A) PRP from healthy donors was pretreated, or not, with 1 μg/mL cyclosporin A (CsA) for 2 h and then treated with TRAP (3 μM). Aggregation was monitored for 5 min. Histograms of maximal aggregation and AUC are shown. Each dot represents a different donor.

(B) Human PRP was pretreated, or not, with 1 μg/mL CsA (CsA hi) or 500 ng/mL CsA (CsA lo) and then stimulated with TRAP (1.5 μM). Integrin αIIbβ3 activation was analyzed by cytofluorimetry. Data show the percentage of the increase of the αIIbβ3 MFI of CsA-treated PRP compared with the αIIbβ3 MFI of PRP not pretreated with CsA. Each dot represents a different donor.

(C) PRP from healthy individual or patients with type 2 or type 1 HPS, as indicated, were pretreated, or not, with 1 μg/mL CsA and then stimulated with TRAP (3 μM). Histograms show platelets' maximal aggregation. Each dot represents an independent test performed on one HPS type 2 patient (left panel) or on two HPS type 1 patients (pz1 and pz2, right panel). Paired t test (A and C) or one-sample t test (B) were used for statistics. *$p < 0.05$, **$p < 0.01$, ***$p < 0.001$. See also Figure S2.

has been reported in patients that use these drugs (Grace et al., 1987; Tomasiak et al., 2007). We observed that NFAT1 dephosphorylation in murine platelets was blocked in the presence of the calcineurin inhibitor FK506 (Figure 1G). Also, that FK506-driven inhibition of the NFAT pathway induced hyperaggregation of murine PRP, as well as washed platelets, exposed to PAR4-AP (Figures 1H and S1I). The calcineurin inhibitor CsA was also able to drive hyperaggregation of mouse platelets (Figure S1J).

FK506-treated platelets displayed enhanced αIIbβ3 integrin activation upon stimulation of the thrombin receptor compared with controls (Figure 1I), but FK506 administration did not affect the activation of αIIbβ3 integrin in cells not exposed to PAR4-AP (Figure 1I). These data demonstrate that calcineurin inhibition does not induce a spontaneous activation of platelets. An increase in the activation of αIIbβ3 integrin in FK506-treated platelets upon PAR4A-AP exposure was also confirmed by an augmented spread of the cells on fibrinogen (Figure S1K). Lastly, calcineurin inhibition did not alter αIIbβ3 integrin activation in *Nfat1*$^{-/-}$ platelets (Figure 1J), demonstrating that the phenotype observed with calcineurin inhibitors is driven by the inhibition of NFAT activation and not by influencing other possible calcineurin targets.

Collectively, these data demonstrate that platelets express several transcription factors of the NFAT family and that calcineurin-dependent dephosphorylation of NFAT, triggered by the activation of the thrombin receptor, diminishes platelet aggregation. Also, that this pathway can be pharmacologically inhibited by commercially available drugs.

NFAT inhibition potentiates the aggregation of human hypoactive platelets

Next, we tested how calcineurin inhibitors affect the response of human platelets to PAR stimulation. As with murine platelets, inhibition of the NFAT pathway in PAR-stimulated human platelets enhanced aggregation compared with that in controls (Figures 2A and S2A). This hyperaggregation phenotype correlated with the increased αIIbβ3 integrin activation (Figure 2B), confirming that inhibition of NFAT in activated human and mouse platelets enhances their aggregation. Thus, the inhibition of this pathway offers the opportunity for therapeutic intervention in human life-threatening pathologies that are characterized by platelet hypoaggregation (Cattaneo, 2013a). To explore this possibility, we assessed the aggregation response in platelets from Hermansky-Pudlak syndrome (HPS) and Glanzmann thrombasthenia (GT) patients. Calcineurin inhibition significantly increased the percentage of maximal aggregation reached by platelets from type 2 and type 1 HPS patients (Figure 2C), as well as from a GT patient (Figure S2B), although the maximal aggregation capacity of hypoactive platelets remained limited compared with the response of platelets derived from healthy donors. Moreover, hyperaggregation in type 2 HPS correlated with increased activation of αIIbβ3 integrin (Figure S2C), as previously observed in healthy donor platelets (Figure 2B).

In sum, although the limited number of subjects tested in our studies mandates the implement of a bigger cohort of patients and requires further clinical studies, inhibition of the NFAT pathway in human platelets may offer a potential therapeutic strategy for dysfunctional platelet pathologies with no currently available specific treatment.

NFAT inhibition increases platelet aggregation *in vivo*

Next, we explored whether interfering with the NFAT pathway by inhibiting NFAT activation *in vivo* can be used as a pre-clinical model for platelet aggregation. Mice were treated with FK506 for 14 days and then their platelet aggregation was tested *ex vivo*. As with the *in vitro* treatment, thrombin receptor stimulation of platelets isolated from FK506-treated mice led to increased aggregation, compared with that of platelets derived from vehicle-treated mice (Figures 3A, S3A, and S3B), demonstrating that *in vivo* administration of a calcineurin inhibitor affects the capacity of platelet to aggregate in response to PAR stimulation.

We then analyzed the effect of inhibiting the NFAT pathway on hemostasis and thrombosis. Blocking activation of NFAT, either chemically (via FK506 treatment of WT mice) or genetically (with use of *Nfat1*$^{-/-}$ mice) resulted in a shorter tail bleeding time relative to that in controls (Figure 3B). Inhibition of the NFAT pathway *in vivo* also exacerbated pulmonary thromboembolism

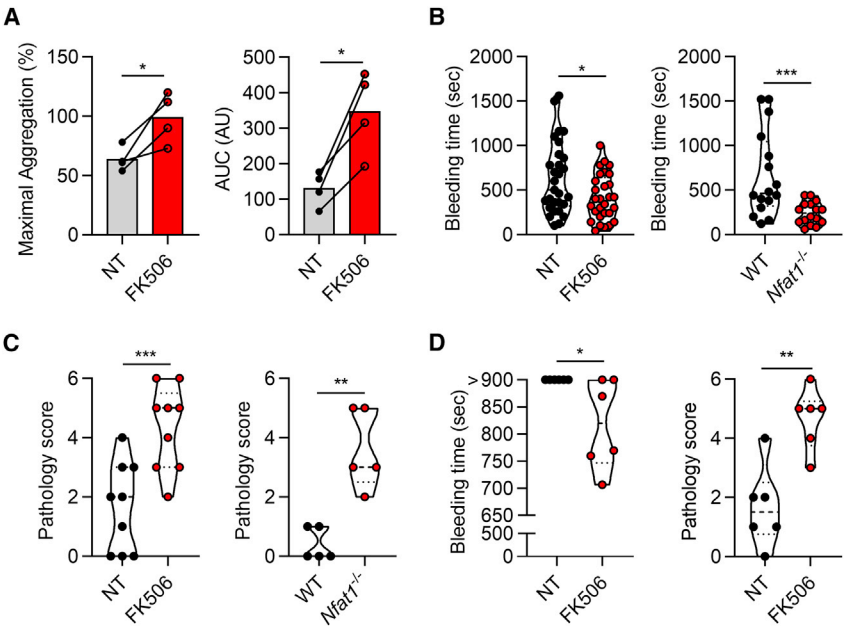

Figure 3. NFAT inhibition increases platelet aggregation *in vivo*

(A) PRP from mice treated, or not, with 4 mg/kg of FK506 for 14 days were stimulated with PAR4-AP (150 μM). Maximal aggregation and AUC are shown. Each dot represents an independent test and lines highlight measurements performed concomitantly.

(B) Tail bleeding test was performed on mice treated, or not, with FK506 (left panel) or on WT and *Nfat1*$^{-/-}$ mice (right panel). Each dot represents a mouse (n = 29 for FK-treated mice, n = 16 for *Nfat1*$^{-/-}$ mice).

(C) Mice treated, or not, with 4 mg/kg of FK506 for 14 days (left) or WT and *Nfat1*$^{-/-}$ mice (right) were intravenously injected with a mixture of collagen (500 μg/kg) and epinephrine (3 μg/kg) and were scored for a pathology index. Each dot represents a mouse (n = 9 for FK-treated mice, n = 5 for *Nfat1*$^{-/-}$ mice).

(D) Tail bleeding test (left panel) and thromboembolism test (right panel) were performed on HPS mice treated, or not, with FK506. Each dot represents a mouse (n = 6). Unpaired two-tailed t test was used for statistics. *$p < 0.05$, **$p < 0.01$, and ***$p < 0.001$. See also Figure S3.

(Figure 3C). The capacity of NFAT inhibition to increase the functionality of hypoactive platelets was confirmed *in vivo* by using HPS mice (Feng et al., 2000). The bleeding time was reduced, and thromboembolism symptoms were increased when HPS mice were treated with FK506, compared with mice in which NFAT activation was left unaltered (Figure 3D). Taken together, these results confirm that NFAT activation *in vivo* physiologically regulates platelet aggregation, whereas NFAT inhibition leads to a hyperactivated phenotype of platelets as also observed *in vitro*, potentially offering a promising modality for treating patients with hyporesponsive platelet disorders.

NFAT tunes the interaction between platelets and neutrophils

Platelet aggregation not only controls hemostasis but is also critical for regulating the interaction of platelets with other immune cells. In particular, platelet-neutrophil complexes serve key pathophysiological roles, facilitating NET induction that, in turn, favors disseminated coagulation and organ failure (Deppermann and Kubes, 2018; Lisman, 2018). Thus, we evaluated whether NFAT inhibition can interfere with the interaction between platelets and neutrophils and, thereby, modulate the functions of these granulocytes. WT mice were treated, or not, with FK506 for 2 weeks, and whole blood was stimulated, or not, *in vitro* with the PAR4-AP. Ly6G^{+} neutrophils displayed an increased signal intensity of the platelet-specific CD41 marker, when blood was derived from the FK506-treated mice compared that from untreated mice (Figure 4A), suggesting that the number of platelets that bind to a single neutrophil is higher in FK506-treated samples. To verify that NFAT inhibition fosters the capacity of platelets to physically interact with neutrophils, we visualized the binding of platelets to single neutrophils. To avoid the possibility that other blood cell functions are altered by FK506, the experiment was performed in blood samples that were depleted of platelets and in which platelets that were treated, or not, *in vitro* with FK506 were added to the same sample. We found that PAR-stimulated platelets in which NFAT activation was inhibited exhibited an increased capacity to interact with neutrophils compared with those in which NFAT was active (Figure 4B). Finally, to establish whether boosting platelet-neutrophil complexes via NFAT inhibition impacts the formation of NETs, we showed that NFAT pathway inhibition (Figure 4C), as well as NFAT1-deficiency (Figure S4A), in PAR4-AP-activated platelets induced a more efficient release of NETs *in vitro*. These results demonstrate that NFAT activation in platelets dampens their capacity to establish physical contacts with neutrophils and NETosis.

A major regulator of the cross talk between platelets and neutrophils is the interaction of P-selectin on platelets and P-selectin glycoprotein ligand (PSGL)-1 on neutrophils (Etulain et al., 2015). Thus, we tested whether NFAT inhibition in platelets regulates P-selectin exposure from alpha granules to the plasma membrane. P-selectin upregulation was enhanced by stimulating the thrombin receptor when NFAT activity was inhibited in FK506-treated murine platelets (Figure 4D), in CsA-treated human platelets (Figure S4B), as well as in *Nfat1*$^{-/-}$ platelets (Figure S4C). When P-selectin was blocked, platelet-induced NET release was significantly decreased and differences between FK506-treated platelets and untreated ones were abolished (Figure 4E). These data demonstrate that NFAT modulates P-selectin exposure in PAR4-activated platelets and thereby increases NET formation upon interaction with neutrophils.

NFAT inhibition promotes release of platelet granules

Platelet P-selectin is contained in alpha granules. Consistent with the report that alpha granule release and sustained platelet aggregation are primarily governed by the autocrine release of ADP from dense granules (Cattaneo, 2013b), we found that stimulation of FK506-treated platelets, as well as *Nfat1*$^{-/-}$ platelets in the presence or absence of an ADP receptor inhibitor abolished the enhanced upregulation of αIIbβ3 integrin, as well as

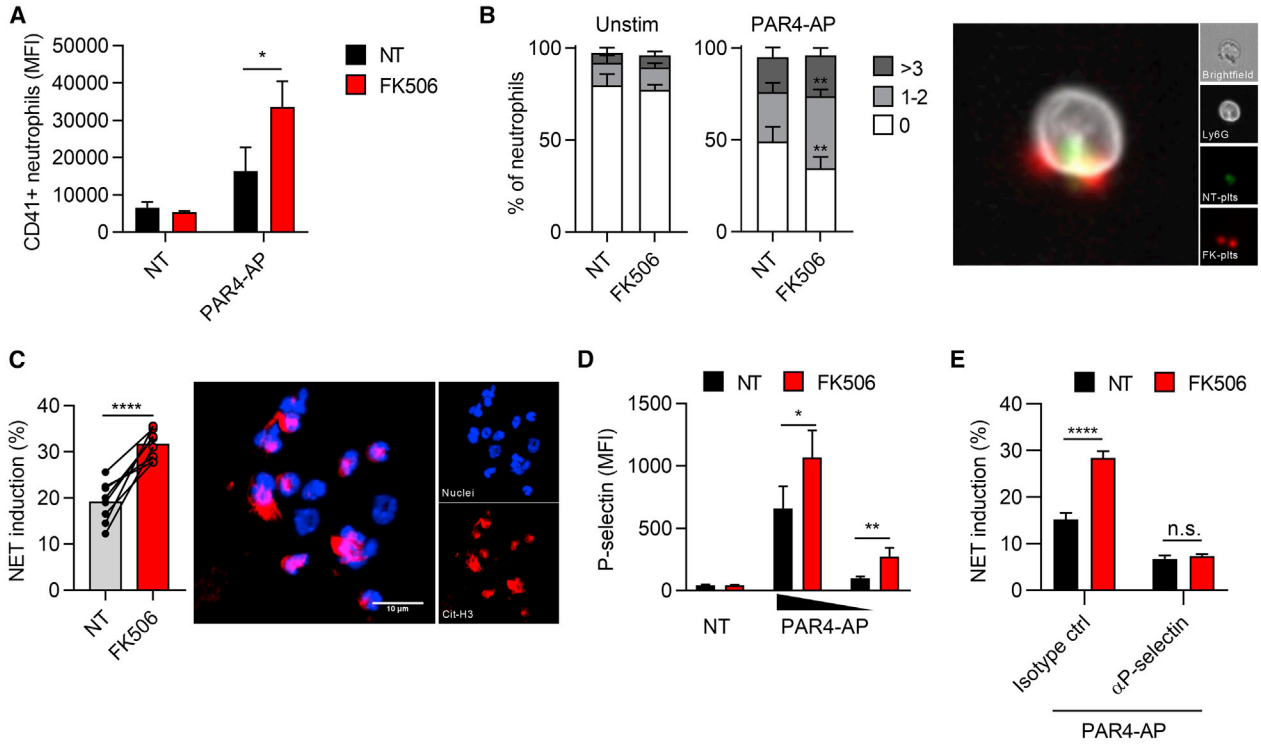

Figure 4. NFAT function governs the interaction between platelets and neutrophils

(A) Whole blood from mice treated, or not, with 4 mg/kg of FK506 for 14 days was stimulated, or not, with PAR4-AP (100 μM). The formation of complexes between platelets and neutrophils was analyzed by cytofluorimetry. Results show the MFI for the platelet marker CD41 on neutrophils, identified as $Ly6G^+CD11b^+$ cells. Data represent mean ± SEM. n ≥ 3 independent experiments.

(B) Platelet-neutrophil complex formation was analyzed by ImageStream. Platelets treated, or not, with 1 μM FK506 for 1 h and identified with different fluorochromes, were washed, mixed with the blood from platelet-depleted mice, and stimulated (PAR4-AP), or not (Unstim), with PAR4-AP (25 μM). The percentage of neutrophils (identified as $Ly6G^+$ cells in the whole blood) that did not bind any platelets (0), or that bound 1 or 2 platelets (1–2), or 3 or more platelets (>3) was measured for both platelets pretreated (FK-506) or not (NT) with FK506. Data represent mean ± SEM. n ≥ 3 independent experiments.

(C) PRP was pretreated, or not, with 1 μM FK506 for 1 h and stimulated with PAR4-AP (150 μM) for 5 min. PAR4-AP-activated platelets were then used to induce NETosis. Histograms represent the percentage of neutrophils positive for the citrullinated histone H3 (left). Each dot represents an independent test. A representative image of NET released by neutrophils is shown (right). Scale bars, 10 μm.

(D) Murine PRP was pretreated, or not, with 1 μM FK506 for 1 h and then stimulated with different concentration of PAR4-AP (150 and 100 μM). P-selectin exposure was analyzed by cytofluorimetry and P-selectin MFI is shown. Data represent mean ± SEM. n ≥ 3 independent experiments.

(E) Neutrophils were stimulated as in (C) in the presence of the anti-P-selectin antibody or respective isotype control. Data represent mean ± SEM. n ≥ 3 independent experiments. One-way ANOVA (A, D, and E), two-way ANOVA (B), or unpaired two-tailed t test (C) were used for statistics. n.s., not significant ($p > 0.05$), *$p < 0.05$, **$p < 0.01$, and ****$p < 0.0001$. See also Figure S4.

of P-selectin associated with the block of NFAT activity (Figures 5A and S5A). These observations demonstrate that NFAT inhibition augments ADP-dependent responses. Next, we tested if increased ADP responses were due to the augmented release of dense granules. In the absence of a functional NFAT pathway, stimulation of the thrombin receptor led to a greater release of dense granules (measured as ATP release) in murine (Figures 5B, and S5B, and S5C), as well as human (Figure S5D) platelets. Notably, inhibition of the NFAT pathway did not increase the aggregation of platelets (Figure 5C) nor the activation of αIIbβ3 integrin and P-selectin (Figures 5D and S5E) upon ADP receptor stimulation, ruling out a direct effect of NFAT on the signaling cascade initiated by the ADP receptor. Furthermore, adding exogenous ADP abolished the differences in αIIbβ3 integrin activation and P-selectin exposure in platelets in which NFAT activation was or was not prevented (Figure 5E). Overall, these data demonstrate that the higher amount of ADP that is released from platelets when NFAT activation is prevented enables a more robust and more sustained activation of platelets.

Inhibition of NFAT activation in platelets using "iNFATuation" reveals a cell-intrinsic role for NFAT in regulating platelet function

Next, we investigated how interfering with NFAT activation specifically in platelets changes their pathophysiological responses *in vivo*. To block all NFAT isoforms in a cell-type-specific manner, we developed a transgenic mouse model (iNFATuation) in which the expression of the VIVIT peptide, and the reporter protein tdTomato, is under the control of the cre-recombinase (Figure 6A). We bred the iNFATuation mice with Pf4-cre-recombinase transgenic mice in which cre is expressed specifically in platelets (Tiedt et al., 2007) (iNFATuation-Pf4-cre from now on) and confirmed that among blood cells only platelets expressed the reporter protein (Figures 6B and S6A). The number of

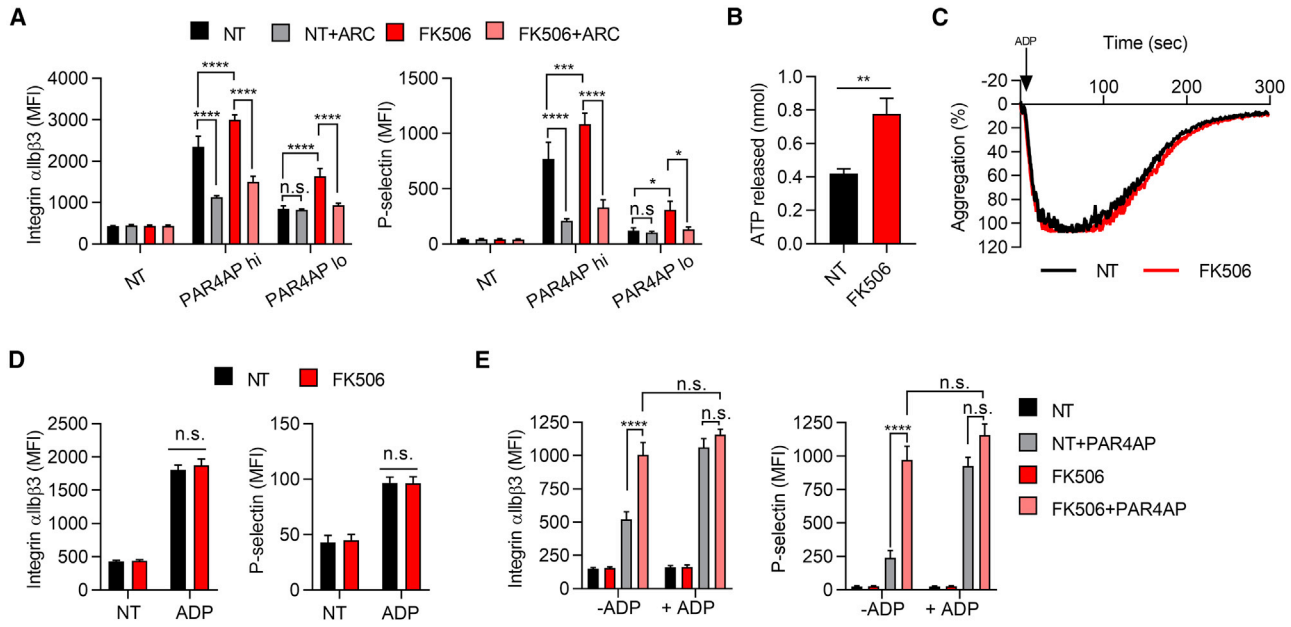

Figure 5. NFAT modulates release of platelet granules

(A) PRP was pretreated, or not, with 1 μM FK506 for 1 h and incubated, or not, for 10 min with 3 μM ARC-66096 (ARC) then stimulated with different concentration of PAR4-AP (150 and 100 μM). Integrin αIIbβ3 activation and P-selectin exposure were analyzed by cytofluorimetry. Bars represent the MFI. Data represent mean ± SEM. n ≥ 3 independent experiments.

(B) PRP was pretreated, or not, with 1 μM FK506 for 1 h and the release of ATP was measured upon stimulation with PAR4-AP (150 μM). Histogram represents maximal ATP release. Data represent mean ± SEM. n ≥ 3 independent experiments.

(C and D) PRP was pretreated as in (B) and then stimulated with ADP (20 μM). Aggregation (C) and integrin αIIbβ3 activation and P-selectin exposure were analyzed (D). Data represent mean ± SEM. n ≥ 3 independent experiments.

(E) PRP was pretreated as in (B) and then stimulated with PAR4-AP (150 μM) alone or in combination with ADP (10 nM). Integrin αIIbβ3 activation and P-selectin exposure were analyzed by cytofluorimetry. Data show mean ± SEM. n ≥ 3 independent experiments. Two-way ANOVA (A, D, and E) or unpaired two-tailed t test (B) were used for statistics. n.s., not significant ($p > 0.05$), *$p < 0.05$, **$p < 0.01$, and ****$p < 0.0001$. See also Figure S5.

platelets in the blood and the expression of CD40L by platelets was similar between iNFATuation-Pf4-cre mice and littermate controls, (Figure S6B) excluding that specific inhibition of NFAT altered megakaryopoiesis or CD40L expression (Crist et al., 2013; Zaslavsky et al., 2013). Platelets isolated from iNFATuation-Pf4-cre mice and activated *in vitro* with PAR4-AP showed reduced NFAT1 dephosphorylation (Figure S6C) and a significant increase in the aggregation and P-selectin expression of activated, but not resting, cells (Figures 6C, 6D, and S6D). Increased formation of heteroaggregates between platelets and neutrophils, as well as potentiated NET induction, where also confirmed when platelets derived from iNFATuation-Pf4-cre, compared to WT, mice were utilized (Figures 6E and 6F). These data demonstrate that the iNFATuation-Pf4-cre mouse model allows the selective inhibition of NFAT activation in platelets and drives platelet hyperresponsiveness.

Thus, we used the iNFATuation-Pf4-cre mice to test how selective NFAT inhibition in platelets affects coagulation *in vivo*. In keeping with the capacity of NFAT to reduce platelet aggregation, we found that iNFATuation-Pf4-cre mice showed increased platelet aggregation as measured by a reduction in the bleeding time and increased severity of thromboembolic events, compared with WT littermates (Figure 6G). Overall, these data confirm a key role for NFAT in platelets to control their functions and demonstrate that the iNFATuation mouse model is a valuable tool to study NFAT inhibition in a cell-type-specific manner.

NFAT inhibition enhances inflammation during septic shock and gram-negative bacterial septicemia

Based on the importance of NFAT activation in platelets in regulating coagulation, interaction with neutrophils and NETosis, we thought to use iNFATuation-Pf4-cre mice to assess how specific NFAT inhibition in platelets affects septic shock or sepsis development. Mice were either injected with two doses of LPS to mimic septic shock or with *Escherichia coli*, to mimic gram-negative bacteria-induced septicemia (Figures 7A and 7B). We found that selective inhibition of NFAT in platelets significantly aggravated the morbidity of iNFATuation-Pf4-cre mice compared with WT littermates as measured by increased temperature drop both during septic shock (Figure 7C) and sepsis (Figure S7A). Next, we tested whether inhibition of NFAT activation in platelets increased disseminated coagulation. To measure disseminated intravascular coagulation, we assessed platelets counts, as reported previously (Wu et al., 2019; Yang et al., 2019), and found a significant reduction in the numbers of platelets in the blood of iNFATuation-Pf4-cre mice, compared with WT littermates, undergoing septic shock (Figure 7D) or sepsis (Figure S7B). Increased disseminated coagulation was further confirmed by a significant decrease in fibrinogen in plasma and/or a significant increase in the formation of thrombin-antithrombin complexes in iNFATuation-Pf4-cre mice, compared with WT littermates, in both inflammatory models (Figures 7E, 7F, S7C, and S7D). In keeping with a detrimental feedback loop between platelets aggregation, platelet-neutrophil

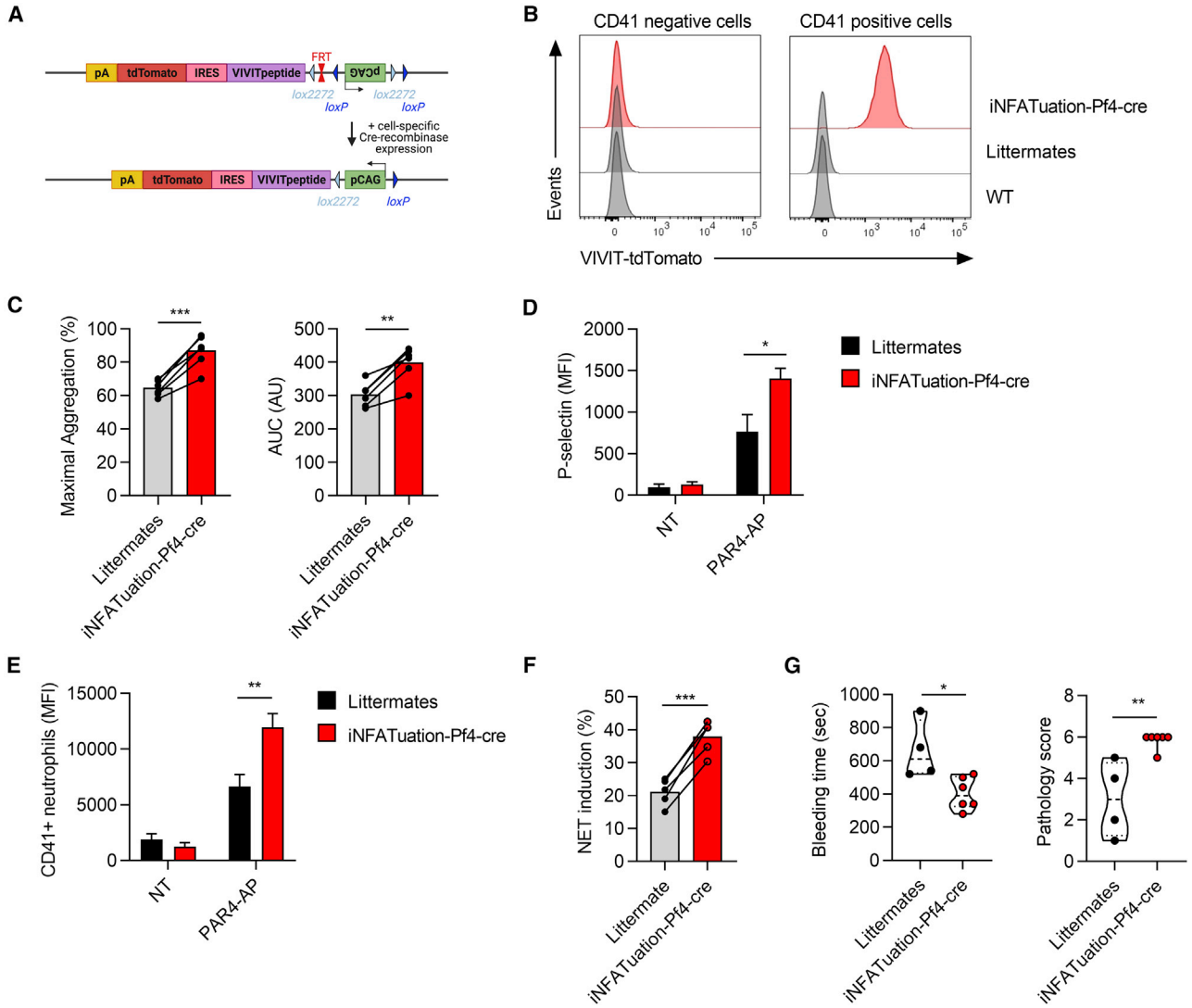

Figure 6. The iNFATuation model demonstrates that NFAT activation in platelets regulates platelet functions

(A) Schematic of the iNFATuation transgenic mouse model.

(B) Blood from WT, littermates or iNFATuation-Pf4-cre mice was stained for the platelet marker CD41 and analyzed for expression of VIVIT-tdTomato signal. One experiment representative of three experiments.

(C) PRP from littermates or iNFATuation-Pf4-cre mice was stimulated with PAR4-AP (150 μM). Aggregation was monitored for 5 min. Histograms of maximal aggregation and AUC are shown. Each dot represents an independent test.

(D) PRP from littermates or iNFATuation-Pf4-cre mice was stimulated with PAR4-AP (150 μM). P-selectin exposure was analyzed by cytofluorimetry, and P-selectin MFI is shown. Data represent mean ± SEM. n ≥ 3 independent experiments.

(E) Whole blood from littermates or iNFATuation-Pf4-cre mice was treated with PAR4-AP (100 μM). The formation of complexes between platelets and neutrophils was analyzed by cytofluorimetry. Results show the MFI for the platelet marker CD41 on neutrophils, identified as $Ly6G^{+}CD11b^{+}$ cells. Data represent mean ± SEM. n ≥ 3 independent experiments.

(F) PRP from littermates or iNFATuation-Pf4-cre mice was stimulated with PAR4-AP (150 μM) for 5 min. PAR4-AP-activated platelets were then used to induce NETosis. Histograms represent the percentage of neutrophils positive for the citrullinated histone H3. Each dot represents an independent test.

(G) Tail bleeding test (left panel) and thromboembolism test (right panel) were performed on littermates or iNFATuation-Pf4-cre mice. Each dot represents a mouse (n = 4 littermates, n = 6 iNFATuation-Pf4-cre). Data show mean ± SEM. Unpaired two-tailed t test (C, F, and G) and two-way ANOVA (D and E) were used for statistics. *p < 0.05, **p < 0.01, and ***p < 0.001. See also Figure S6.

interactions and NETosis, we also found increased formation of platelet-neutrophil heterocomplexes, and/or augmented formation of NETs (measured by histone H3 citrullination on neutrophils (Poli et al., 2021)) in iNFATuation-Pf4-cre mice, compared with WT littermates, both during septic shock or septicemia (Figures 7G, 7H, and S7E). Numbers of neutrophils either in the peritoneal cavity or the blood were not significantly different in iNFATuation-Pf4-cre mice or littermates either during sepsis or septic shock (Figures S7F–S7J). In keeping with an increased inflammatory state driven by the negative feedback loop initiated by the interaction between

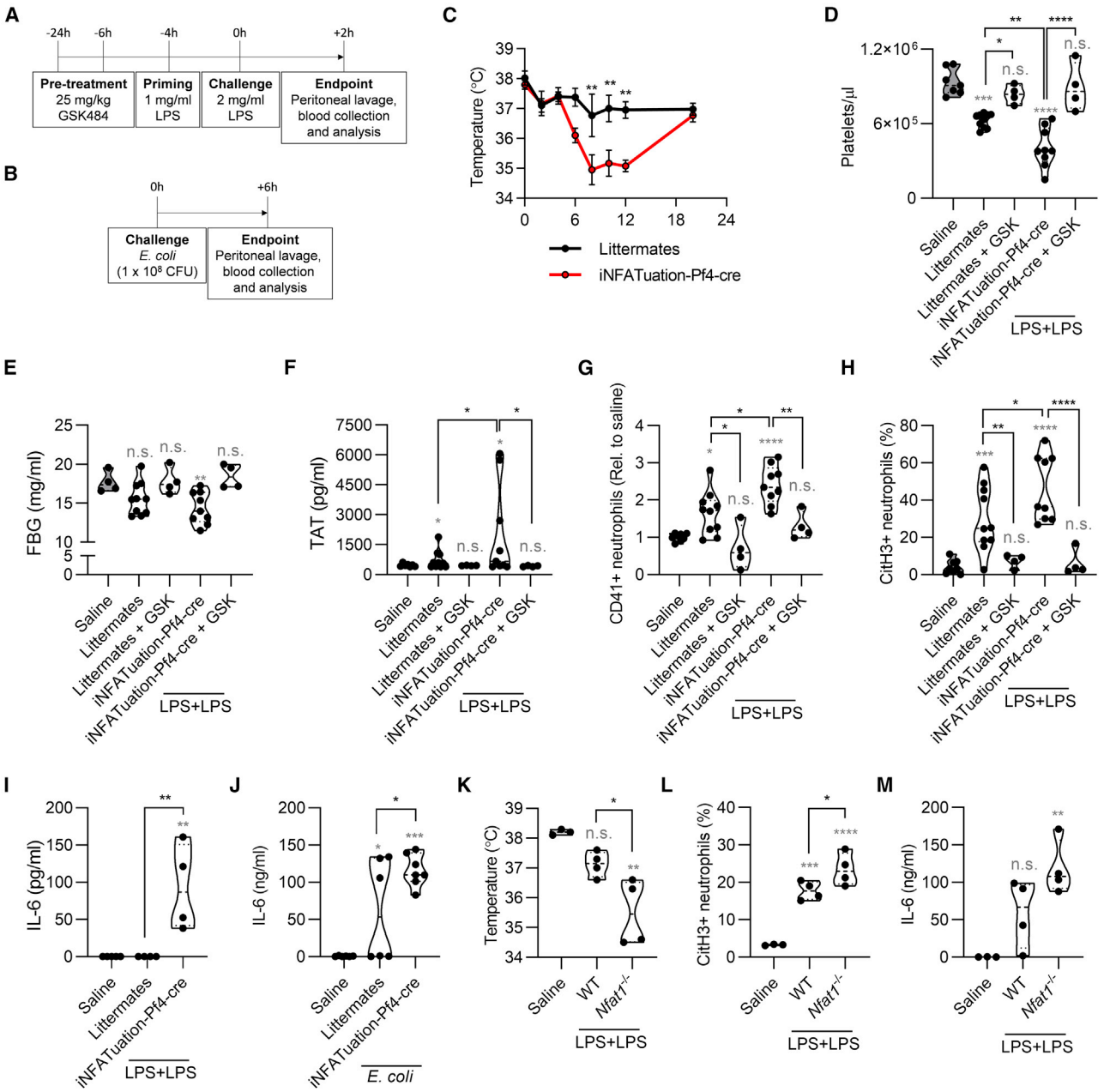

Figure 7. NFAT inhibition exacerbates inflammation during sepsis

(A) Schematic of the septic shock model. Mice were intraperitoneally (i.p.) injected, or not, with 25 mg/kg of GSK484 (−24 h and −6 h) and then were i.p. administered with two doses of LPS (−4 h, 1 mg/kg and 0 h, 2 mg/kg) to induce septic shock. Peritoneal lavage and blood were collected 2 h after the LPS challenge.

(B) Schematic of gram-negative bacteria-induced sepsis. Mice were i.p. injected with 1 × 10^8 CFU of *E. coli*. Peritoneal lavage and blood were collected 6 h after the *E. coli* challenge.

(C) Littermates or iNFATuation-Pf4-cre mice were challenged with two doses of LPS (−4 h, 1 mg/kg and 0 h, 2 mg/kg). Temperatures were recorded at the indicated time points. n = 4 mice per group. Data show mean ± SEM.

(D–I) Littermates or iNFATuation-Pf4-cre mice were pretreated, or not, with GSK484 and then challenged with two doses of LPS. 2 h after LPS challenge blood was collected, platelet number (D) was assessed by cytofluorimetry, and plasma fibrinogen content (E) and thrombin-antithrombin complexes (F) were measured by ELISA. Neutrophils positive for platelet marker CD41 (G) and for citrullinated histone H3 (H) were quantified in the peritoneal lavage by cytofluorimetry. Plasma IL-6 content was measured by ELISA 18 h post challenge (I). Each dot represents a mouse. "Saline" are WT mice not challenged with LPS used as control.

(J) Littermates or iNFATuation-Pf4-cre mice were challenge with 1 × 10^8 CFU of *E. coli*. 6 h post infection, plasma IL-6 was quantified by ELISA. Each dot represents a mouse. "Saline" are WT mice not challenged with *E. coli* used as control.

(legend continued on next page)

platelets and neutrophils, we also found increased IL-6 in the blood of iNFATuation-Pf4-cre mice compared with WT littermates, treated with either LPS or *E. coli* (Figures 7I and 7J). To formally demonstrate these changes are mainly due to increased NET formation secondary to NFAT inhibition in platelets, in the septic shock model we also utilized the drug GSK484 that specifically inhibits histone H3 citrullination, thus preventing NETosis (Poli et al., 2021; Thiam et al., 2020). We confirmed, for all the parameters previously measured, that NET inhibition efficiently blocked the pro-inflammatory feedback loop between NFAT-inhibited platelets and neutrophils (Figures 7D–7H and S7I–S7L). We also found increased morbidity, NETosis, and pro-inflammatory cytokine production in WT mice depleted of endogenous platelets and transfused with *Nfat1*$^{-/-}$ platelets before LPS-induced septic shock (Figures 7K–7M). Finally, increased NETosis was also visualized in the peritoneum of *E. coli*-injected mice previously depleted of endogenous platelets and transplanted with either FK506-treated or *Nfat1*$^{-/-}$ platelets (Figures S7M and S7N). These results confirm that the NFAT pathway modulates the ability of platelets to instruct and sustain the immune response during sepsis and raise the possibility to develop future therapeutic approaches aimed at potentiating NFAT activation in platelets as an intervention against sepsis.

DISCUSSION

Platelets were first discovered for their fundamental role in hemostasis and thrombosis, and for many years these highly specialized cells were believed to have evolved in mammals to serve the exclusive role of patrolling the vessel endothelium and to repair it in case of damage. In contrast, in other metazoa, a single type of circulating nucleated cell is responsible for all defensive mechanisms, including hemostasis, as well as immune functions. Over the last decade, mammalian platelets have also been shown to play a key role during an immune response (Dinkla et al., 2016; Han et al., 2020; Rolfes et al., 2020; Rossaint et al., 2016; Sreeramkumar et al., 2014). Here, we document that NFAT activation in platelets serves as a fundamental checkpoint that regulates not only platelet hemostatic functions but also their immunological roles. These data demonstrate that transcription factors can serve non-transcriptional roles in the pathophysiology of anucleated cells.

Our data further show that pharmacological inhibition of the NFAT pathway partly rescues functional defects of platelets from patients with hyporesponsive platelet diseases, such as HPS and GT. Unveiling this function for a well-known immune player, such as NFAT, identifies a potential therapeutic target for modulating platelet activity. Currently available drugs are solely focused on inhibiting platelet responses; to our knowledge, there is no efficacious drug that directly improves platelet functionality. Boosting platelet responses *in vivo* could be extremely useful in developing treatments for hyporesponsive platelet pathologies, such as HPS and GT, for which effective treatments are still lacking. Although the inhibitors of NFAT activation that we studied—FK506 (also known as tacrolimus) and CsA—are already commercially available drugs, their efficacy in restoring aggregation of hypofunctional platelets derived from patients is only partial and more efficient drugs may be developed in the future.

Given the peculiar and diverse functions of platelets (Nicolai et al., 2019; Yeaman, 2014), these cells represent a bridge between thrombotic and inflammatory pathways. Here, we show that the hyperactivated phenotype induced in platelets by inhibition of the NFAT pathway results in a greater ability of these cells to interact with neutrophils and stimulate the release of NETs in *in vitro* and *in vivo* sepsis models. Hyperactivation of platelets exacerbates endotoxic shock and gram-negative bacteria-driven septicemia, drives massive NETs release, and leads to a poor outcome. These results corroborate the notion of a strong platelet-neutrophil relationship and underscore the critical importance of regulating this interaction under pathophysiological conditions. Further studies are needed to identify compounds that can sustain and/or induce NFAT activation specifically in platelets and that can be used to intervene against sepsis.

From a molecular perspective, our results demonstrate that NFAT is a negative regulator of platelet response. A key unanswered question is how this transcription factor exerts its non-genomic function. In nucleated cells, cytosolic NFAT is part of a multi-protein complex that is necessary to precisely tune NFAT dephosphorylation and activation (Sharma et al., 2011). Some of the proteins that interact with NFAT in nucleated cells are also present in platelets, where they serve specific functions in modulating platelet activation (Bahou et al., 2004; Li et al., 2008; Steele et al., 2009). We argue that NFAT functions serve as molecular hubs in platelets that, upon thrombin receptor stimulation, enable the activation and/or inhibition of downstream effectors by determining their availability and functionality. Our data with use of Nfat1$^{-/-}$ platelets, chemical inhibitors of calcineurin, platelets transiently exposed to the VIVIT peptide, as well as platelets derived from the iNFATuation mouse model that constitutively express the VIVIT peptide suggest that the presence of NFAT, and the ability of NFAT to be dephosphorylated, are critical in the modulation of platelet activation. Dephosphorylated NFAT likely acts either by capturing and turning off positive regulators of the platelet activation cascade, or by releasing inhibitory proteins that turn off the platelet response. Although further studies are needed to determine the exact molecular mechanism that underlies the non-genomic role of NFAT, our discovery of a non-transcriptional role of NFAT unveils an additional layer of complexity in NFAT biology, which must be accounted for when considering the numerous side effects of calcineurin inhibition as an immunosuppressive treatment, as well as when defining strategies to intervene against life-threatening disorders that involve platelet activation.

Finally, our results have uncovered a non-transcriptional role of the transcription factor NFAT, raising the possibility that even in nucleated cells NFAT could have a non-genomic role

(K–M) Platelet-depleted mice reconstituted with WT or *Nfat1*$^{-/-}$ platelets were challenged with 2 doses of LPS. 2 h after LPS challenge temperatures were recorded (K), percentage of neutrophils positive for citrullinated histone H3 were analyzed from the peritoneum by cytofluorimetry (L), and plasma IL-6 concentration was measured by ELISA (M). Each dot represents a mouse. "Saline" are WT mice not challenged with LPS used as control. Two-way ANOVA (A), and one-way ANOVA (D–M) were used for statistics. n.s., not significant ($p > 0.05$), *$p < 0.05$, **$p < 0.01$, ***$p < 0.001$, and ****$p < 0.0001$. In (D–M) gray stars represent statistics compared with saline group. See also Figure S7.

that has, to date, been overlooked. Cell types characterized by the expression of NFAT, and those that exhibit the capacity to activate rapid, transcription-independent responses, hold promise for further exploring non-transcriptional roles of NFAT also in nucleated cells. The iNFATuation mouse model that we developed may serve as a valuable tool in the future to study these non-canonical, as well as more canonical, functions of NFAT.

Limitations of the study

We assessed the relevance of NFAT activation in platelets employing mouse models of LPS-driven septic shock or *E. coli*-driven septicemia, but how the activation of the NFAT pathway in platelets may affect polymicrobial sepsis, i.e., in the cecum ligation and punction model, remains still to be determined.

Our data using a multi-pronged approach based on the use of commercially available drugs, NFAT1-deficient mice, a cell-permeable form of the VIVIT peptide, as well as the iNFATuation mouse model we developed support the hypothesis that activation of NFAT in platelets is a fundamental checkpoint of platelet activation and functions. Nevertheless, each single approach presents some limitations: (1) FK506 and CsA are known to interact and alter the activity of different cyclophilins and to generically inhibit calcineurin activities not only related to NFAT activation; (2) use of mice and cells derived from NFAT1-deficient mice are limited by the fact that only one of the NFAT family members is missing, leaving unexplored possible additional layer of complexity driven by the cross talk between different NFAT forms. Also, the mice are total knockouts and NFAT-deficiency in other cell types may also contribute to altered platelet functionality; (3) although the VIVIT peptide has been selected to specifically block calcineurin and NFAT interaction (Aramburu et al., 1999), it is impossible to exclude bystander targets may also be affected by this peptide. Of note, possible effect of constitutive, rather than acute, NFAT inhibition or deficiency may alter megakaryocyte activities, which have been previously shown to rely on the calcineurin and NFAT pathway for some of their functions (Arabanian et al., 2012; Crist et al., 2013; Zaslavsky et al., 2013). However, we believe that the fact all the approaches utilized in the present work led to the same conclusions demonstrates the key role played by NFAT in regulating the pathophysiological functions of platelets.

Finally, although we have proved that NFAT inhibition in activated platelets exacerbates their activation, aggregation, and interaction with neutrophils, once drugs capable of activating NFAT in platelets will be available it will be important to test their capacity to improve septicemia to pose the base for novel ways of therapeutic intervention.

STAR★METHODS

Detailed methods are provided in the online version of this paper and include the following:

SUPPLEMENTAL INFORMATION

Supplemental information can be found online at https://doi.org/10.1016/j.immuni.2021.12.002.

ACKNOWLEDGMENTS

I.Z. is supported by NIH grants R01AI121066, R01DK115217, R01AI165505, and NIAID-DAIT-NIHAI201700100; Lloyd J. Old STAR Program CRI3888; and holds an Investigators in the Pathogenesis of Infectious Disease Award from the Burroughs Wellcome Fund. F.G. is supported by AIRC (IG 2019Id.23512), Fondazione regionale per la ricerca Biomedica, FRRB (IANG-CRC CP2_12/2018), and Ministero della Salute, Ricerca Finalizzata (RF-2018-12367072).

AUTHOR CONTRIBUTIONS

V.P. designed, performed, and analyzed the experiments and wrote the paper; M.D.G. contributed to perform and analyze *in vivo* experiments; M.S.-V., A.L.F., A.D.M., and F.G. contributed to design the experiments; I.Z. conceived the project, designed the experiments, wrote the paper, and supervised the study.

DECLARATION OF INTERESTS

The authors declare no competing interests.

INCLUSION AND DIVERSITY

We worked to ensure sex balance in the selection of non-human subjects. We worked to ensure diversity in experimental samples through the selection of the cell lines. While citing references scientifically relevant for this work, we also actively worked to promote gender balance in our reference list. The author list of this paper includes contributors from the location where the research was conducted who participated in the data collection, design, analysis, and/or interpretation of the work.

Received: February 9, 2021
Revised: September 9, 2021
Accepted: December 3, 2021
Published: January 6, 2022

REFERENCES

Adrover, J.M., Aroca-Crevillén, A., Crainiciuc, G., Ostos, F., Rojas-Vega, Y., Rubio-Ponce, A., Cilloniz, C., Bonzón-Kulichenko, E., Calvo, E., Rico, D., et al. (2020). Programmed "disarming" of the neutrophil proteome reduces the magnitude of inflammation. Nat. Immunol. *21*, 135–144.

Akbiyik, F., Ray, D.M., Gettings, K.F., Blumberg, N., Francis, C.W., and Phipps, R.P. (2004). Human bone marrow megakaryocytes and platelets express PPARgamma, and PPARgamma agonists blunt platelet release of CD40 ligand and thromboxanes. Blood *104*, 1361–1368.

Arabanian, L.S., Kujawski, S., Habermann, I., Ehninger, G., and Kiani, A. (2012). Regulation of fas/fas ligand-mediated apoptosis by nuclear factor of activated T cells in megakaryocytes. Br. J. Haematol. *156*, 523–534.

Aramburu, J., Yaffe, M.B., López-Rodríguez, C., Cantley, L.C., Hogan, P.G., and Rao, A. (1999). Affinity-driven peptide selection of an NFAT inhibitor more selective than cyclosporin A. Science *285*, 2129–2133.

Azzi, J.R., Sayegh, M.H., and Mallat, S.G. (2013). Calcineurin inhibitors: 40 years later, can't live without. J. Immunol. *191*, 5785–5791.

Bahou, W.F., Scudder, L., Rubenstein, D., and Jesty, J. (2004). A shear-restricted pathway of platelet procoagulant activity is regulated by IQGAP1. J. Biol. Chem. *279*, 22571–22577.

Bennett, J.S. (2005). Structure and function of the platelet integrin alphaIIbbeta3. J. Clin. Invest. *115*, 3363–3369.

Brinkmann, V., Reichard, U., Goosmann, C., Fauler, B., Uhlemann, Y., Weiss, D.S., Weinrauch, Y., and Zychlinsky, A. (2004). Neutrophil extracellular traps kill bacteria. Science *303*, 1532–1535.

Carestia, A., Kaufman, T., Rivadeneyra, L., Landoni, V.I., Pozner, R.G., Negrotto, S., D'Atri, L.P., Gómez, R.M., and Schattner, M. (2016). Mediators and molecular pathways involved in the regulation of neutrophil extracellular trap formation mediated by activated platelets. J. Leukoc. Biol. *99*, 153–162.

Cattaneo, M. (2013a). Congenital disorders of platelet function. In Platelets (Academic press), pp. 1019–1047.

Cattaneo, M. (2013b). The platelet P2 receptors. In Platelets (Academic press), pp. 261–281.

Clark, S.R., Ma, A.C., Tavener, S.A., McDonald, B., Goodarzi, Z., Kelly, M.M., Patel, K.D., Chakrabarti, S., McAvoy, E., Sinclair, G.D., et al. (2007). Platelet TLR4 activates neutrophil extracellular traps to ensnare bacteria in septic blood. Nat. Med. *13*, 463–469.

Cohen, J. (2002). The immunopathogenesis of sepsis. Nature *420*, 885–891.

Crist, S.A., Elzey, B.D., Ahmann, M.T., and Ratliff, T.L. (2013). Early growth response-1 (EGR-1) and nuclear factor of activated T cells (NFAT) cooperate to mediate CD40L expression in megakaryocytes and platelets. J. Biol. Chem. *288*, 33985–33996.

Deng, M., Tang, Y., Li, W., Wang, X., Zhang, R., Zhang, X., Zhao, X., Liu, J., Tang, C., Liu, Z., et al. (2018). The endotoxin delivery protein HMGB1 mediates caspase-11-dependent lethality in sepsis. Immunity *49*, 740–753, e7.

Deppermann, C., and Kubes, P. (2018). Start a fire, kill the bug: the role of platelets in inflammation and infection. Innate Immun *24*, 335–348.

Dinkla, S., van Cranenbroek, B., van der Heijden, W.A., He, X., Wallbrecher, R., Dumitriu, I.E., van der Ven, A.J., Bosman, G.J., Koenen, H.J., and Joosten, I. (2016). Platelet microparticles inhibit IL-17 production by regulatory T cells through P-selectin. Blood *127*, 1976–1986.

Elaskalani, O., Abdol Razak, N.B., and Metharom, P. (2018). Neutrophil extracellular traps induce aggregation of washed human platelets independently of extracellular DNA and histones. Cell Commun. Signal. *16*, 24.

Etulain, J., Martinod, K., Wong, S.L., Cifuni, S.M., Schattner, M., and Wagner, D.D. (2015). P-selectin promotes neutrophil extracellular trap formation in mice. Blood *126*, 242–246.

Feng, L., Rigatti, B.W., Novak, E.K., Gorin, M.B., and Swank, R.T. (2000). Genomic structure of the mouse Ap3b1 gene in normal and pearl mice. Genomics *69*, 370–379.

Grace, A.A., Barradas, M.A., Mikhailidis, D.P., Jeremy, J.Y., Moorhead, J.F., Sweny, P., and Dandona, P. (1987). Cyclosporine A enhances platelet aggregation. Kidney Int *32*, 889–895.

Hagar, J.A., Powell, D.A., Aachoui, Y., Ernst, R.K., and Miao, E.A. (2013). Cytoplasmic LPS activates caspase-11: implications in TLR4-independent endotoxic shock. Science *341*, 1250–1253.

Han, P., Hanlon, D., Arshad, N., Lee, J.S., Tatsuno, K., Robinson, E., Filler, R., Sobolev, O., Cote, C., Rivera-Molina, F., et al. (2020). Platelet P-selectin initiates cross-presentation and dendritic cell differentiation in blood monocytes. Sci. Adv. *6*, eaaz1580.

Jackson, S.P., Darbousset, R., and Schoenwaelder, S.M. (2019). Thromboinflammation: challenges of therapeutically targeting coagulation and other host defense mechanisms. Blood *133*, 906–918.

Jimenez-Alcazar, M., Rangaswamy, C., Panda, R., Bitterling, J., Simsek, Y.J., Long, A.T., Bilyy, R., Krenn, V., Renne, C., Renne, T., et al. (2017). Host DNases prevent vascular occlusion by neutrophil extracellular traps. Science *358*, 1202–1206.

Kayagaki, N., Stowe, I.B., Lee, B.L., O'Rourke, K., Anderson, K., Warming, S., Cuellar, T., Haley, B., Roose-Girma, M., Phung, Q.T., et al. (2015). Caspase-11 cleaves gasdermin D for non-canonical inflammasome signalling. Nature *526*, 666–671.

Kayagaki, N., Wong, M.T., Stowe, I.B., Ramani, S.R., Gonzalez, L.C., Akashi-Takamura, S., Miyake, K., Zhang, J., Lee, W.P., Muszyński, A., et al. (2013). Noncanonical inflammasome activation by intracellular LPS independent of TLR4. Science *341*, 1246–1249.

Khatlani, T., Pradhan, S., Da, Q., Gushiken, F.C., Bergeron, A.L., Langlois, K.W., Molkentin, J.D., Rumbaut, R.E., and Vijayan, K.V. (2014). The beta isoform of the catalytic subunit of protein phosphatase 2B restrains platelet function by suppressing outside-in alphaII b beta3 integrin signaling. J. Thromb. Haemost. *12*, 2089–2101.

Lannan, K.L., Sahler, J., Kim, N., Spinelli, S.L., Maggirwar, S.B., Garraud, O., Cognasse, F., Blumberg, N., and Phipps, R.P. (2015). Breaking the mold: transcription factors in the anucleate platelet and platelet-derived microparticles. Front. Immunol. *6*, 48.

Li, D., August, S., and Woulfe, D.S. (2008). GSK3beta is a negative regulator of platelet function and thrombosis. Blood *111*, 3522–3530.

Li, Z., Delaney, M.K., O'Brien, K.A., and Du, X. (2010). Signaling during platelet adhesion and activation. Arterioscler. Thromb. Vasc. Biol. *30*, 2341–2349.

Lisman, T. (2018). Platelet-neutrophil interactions as drivers of inflammatory and thrombotic disease. Cell Tissue Res *371*, 567–576.

Liu, S., Su, X., Pan, P., Zhang, L., Hu, Y., Tan, H., Wu, D., Liu, B., Li, H., Li, H., et al. (2016). Neutrophil extracellular traps are indirectly triggered by lipopolysaccharide and contribute to acute lung injury. Sci. Rep. *6*, 37252.

Lizio, M., Abugessaisa, I., Noguchi, S., Kondo, A., Hasegawa, A., Hon, C.C., de Hoon, M., Severin, J., Oki, S., Hayashizaki, Y., et al. (2019). Update of the FANTOM web resource: expansion to provide additional transcriptome atlases. Nucleic Acids Res *47*, D752–D758.

Malaver, E., Romaniuk, M.A., D'Atri, L.P., Pozner, R.G., Negrotto, S., Benzadón, R., and Schattner, M. (2009). NF-kappaB inhibitors impair platelet activation responses. J. Thromb. Haemost. *7*, 1333–1343.

McDonald, B., Davis, R.P., Kim, S.J., Tse, M., Esmon, C.T., Kolaczkowska, E., and Jenne, C.N. (2017). Platelets and neutrophil extracellular traps collaborate to promote intravascular coagulation during sepsis in mice. Blood *129*, 1357–1367.

McDonald, B., Urrutia, R., Yipp, B.G., Jenne, C.N., and Kubes, P. (2012). Intravascular neutrophil extracellular traps capture bacteria from the bloodstream during sepsis. Cell Host Microbe *12*, 324–333.

Mócsai, A., Jakus, Z., Vántus, T., Berton, G., Lowell, C.A., and Ligeti, E. (2000). Kinase pathways in chemoattractant-induced degranulation of neutrophils: the role of p38 mitogen-activated protein kinase activated by Src family kinases. J. Immunol. *164*, 4321–4331.

Nicolai, L., Gaertner, F., and Massberg, S. (2019). Platelets in host defense: experimental and clinical insights. Trends Immunol *40*, 922–938.

Poli, V., Pui-Yan Ma, V., Di Gioia, M., Broggi, A., Benamar, M., Chen, Q., Mazitschek, R., Haggarty, S.J., Chatila, T.A., Karp, J.M., and Zanoni, I. (2021). Zinc-dependent histone deacetylases drive neutrophil extracellular

trap formation and potentiate local and systemic inflammation. iScience *24*, 103256.

Rivera, J., Lozano, M.L., Navarro-Núñez, L., and Vicente, V. (2009). Platelet receptors and signaling in the dynamics of thrombus formation. Haematologica *94*, 700–711.

Rolfes, V., Ribeiro, L.S., Hawwari, I., Böttcher, L., Rosero, N., Maasewerd, S., Santos, M.L.S., Próchnicki, T., Silva, C.M.S., Wanderley, C.W.S., et al. (2020). Platelets fuel the inflammasome activation of innate immune cells. Cell Rep *31*, 107615.

Rossaint, J., Kühne, K., Skupski, J., Van Aken, H., Looney, M.R., Hidalgo, A., and Zarbock, A. (2016). Directed transport of neutrophil-derived extracellular vesicles enables platelet-mediated innate immune response. Nat. Commun. *7*, 13464.

Saitoh, T., Komano, J., Saitoh, Y., Misawa, T., Takahama, M., Kozaki, T., Uehata, T., Iwasaki, H., Omori, H., Yamaoka, S., et al. (2012). Neutrophil extracellular traps mediate a host defense response to human immunodeficiency virus-1. Cell Host Microbe *12*, 109–116.

Schnütgen, F., Doerflinger, N., Calléja, C., Wendling, O., Chambon, P., and Ghyselinck, N.B. (2003). A directional strategy for monitoring Cre-mediated recombination at the cellular level in the mouse. Nat. Biotechnol. *21*, 562–565.

Sharma, S., Findlay, G.M., Bandukwala, H.S., Oberdoerffer, S., Baust, B., Li, Z., Schmidt, V., Hogan, P.G., Sacks, D.B., and Rao, A. (2011). Dephosphorylation of the nuclear factor of activated T cells (NFAT) transcription factor is regulated by an RNA-protein scaffold complex. Proc. Natl. Acad. Sci. USA *108*, 11381–11386.

Sreeramkumar, V., Adrover, J.M., Ballesteros, I., Cuartero, M.I., Rossaint, J., Bilbao, I., Nácher, M., Pitaval, C., Radovanovic, I., Fukui, Y., et al. (2014). Neutrophils scan for activated platelets to initiate inflammation. Science *346*, 1234–1238.

Steele, B.M., Harper, M.T., Macaulay, I.C., Morrell, C.N., Perez-Tamayo, A., Foy, M., Habas, R., Poole, A.W., Fitzgerald, D.J., and Maguire, P.B. (2009). Canonical Wnt signaling negatively regulates platelet function. Proc. Natl. Acad. Sci. USA *106*, 19836–19841.

Tang, Y., Wang, X., Li, Z., He, Z., Yang, X., Cheng, X., Peng, Y., Xue, Q., Bai, Y., Zhang, R., et al. (2021). Heparin prevents caspase-11-dependent septic lethality independent of anticoagulant properties. Immunity *54*, 454–467, e6.

Thiam, H.R., Wong, S.L., Wagner, D.D., and Waterman, C.M. (2020). Cellular mechanisms of NETosis. Annu. Rev. Cell Dev. Biol. *36*, 191–218.

Tiedt, R., Schomber, T., Hao-Shen, H., and Skoda, R.C. (2007). Pf4-Cre transgenic mice allow the generation of lineage-restricted gene knockouts for studying megakaryocyte and platelet function *in vivo*. Blood *109*, 1503–1506.

Tomasiak, M., Rusak, T., Gacko, M., and Stelmach, H. (2007). Cyclosporine enhances platelet procoagulant activity. Nephrol. Dial. Transplant. *22*, 1750–1756.

Williams, S.C. (2012). After Xigris, researchers look to new targets to combat sepsis. Nat. Med. *18*, 1001.

Wu, C., Lu, W., Zhang, Y., Zhang, G., Shi, X., Hisada, Y., Grover, S.P., Zhang, X., Li, L., Xiang, B., et al. (2019). Inflammasome activation triggers blood clotting and host death through pyroptosis. Immunity *50*, 1401–1411, e4.

Xu, J., Zhang, X., Pelayo, R., Monestier, M., Ammollo, C.T., Semeraro, F., Taylor, F.B., Esmon, N.L., Lupu, F., and Esmon, C.T. (2009). Extracellular histones are major mediators of death in sepsis. Nat. Med. *15*, 1318–1321.

Yang, X., Cheng, X., Tang, Y., Qiu, X., Wang, Y., Kang, H., Wu, J., Wang, Z., Liu, Y., Chen, F., et al. (2019). Bacterial endotoxin activates the coagulation cascade through gasdermin D-dependent phosphatidylserine exposure. Immunity *51*, 983–996, e6.

Yeaman, M.R. (2014). Platelets: at the nexus of antimicrobial defence. Nat. Rev. Microbiol. *12*, 426–437.

Yost, C.C., Schwertz, H., Cody, M.J., Wallace, J.A., Campbell, R.A., Vieira-de-Abreu, A., Araujo, C.V., Schubert, S., Harris, E.S., Rowley, J.W., et al. (2016). Neonatal NET-inhibitory factor and related peptides inhibit neutrophil extracellular trap formation. J. Clin. Invest. *126*, 3783–3798.

Zanoni, I., and Granucci, F. (2012). Regulation and dysregulation of innate immunity by NFAT signaling downstream of pattern recognition receptors (PRRs). Eur. J. Immunol. *42*, 1924–1931.

Zaslavsky, A., Chou, S.T., Schadler, K., Lieberman, A., Pimkin, M., Kim, Y.J., Baek, K.H., Aird, W.C., Weiss, M.J., and Ryeom, S. (2013). The calcineurin-NFAT pathway negatively regulates megakaryopoiesis. Blood *121*, 3205–3215.

STAR★METHODS

KEY RESOURCES TABLE

REAGENT or RESOURCE	SOURCE	IDENTIFIER
Antibodies		
Anti-NFAT1	Cell Signaling Technology	Cat# 5861 RRID:AB_10834808
Anti-NFAT2	Cell Signaling Technology	Cat# 8032 RRID:AB_10829466
Anti-NFAT3	Cell Signaling Technology	Cat# 2183 RRID:AB_2152912
Anti-NFAT4	Cell Signaling Technology	Cat# 4998 RRID:AB_2152771
Anti-p65	Cell Signaling Technology	Cat# 8242 RRID:AB_10859369
Anti-p38	Cell Signaling Technology	Cat# 8690 RRID:AB_10999090
Anti-p-p38	Cell Signaling Technology	Cat# 4511 RRID:AB_2139682
Anti-Src	Cell Signaling Technology	Cat# 2109 RRID:AB_2106059
Anti-p-Src	Cell Signaling Technology	Cat# 6943 RRID:AB_10013641
Anti-β-actin	Sigma-Aldrich	Cat# A2228 RRID:AB_476697
Anti-citrullinated histone H3	Abcam	Cat# ab5103 RRID:AB_304752
Anti-rabbit Alexa 647	Thermo Fisher	Cat# A27040 RRID:AB_2536101
Anti-mouse Ly6G FITC	BioLegend	Cat# 127605 RRID:AB_1236488
Anti-mouse/human CD11b APC	BioLegend	Cat# 101211 RRID:AB_312794
Anti-mouse/rat CD62P APC	BioLegend	Cat# 148303 RRID:AB_2565272
Anti-mouse CD41 PE-Cy7	BioLegend	Cat# 133915 RRID:AB_11125173
Anti-mouse CD154-FITC	BioLegend	Cat# 157005 RRID:AB_2814085
Anti-human CD62P PE	BioLegend	Cat# 304905 RRID:AB_314477
Anti-human CD42b APC	BioLegend	Cat# 303912 RRID:AB_2113770
Anti-integrin αIIbβ3 (active form) PE	Emfret	Cat# M023-2 RRID:AB_2833084
Anti-PAC1 FITC	BD Bioscience	Cat# 340507 RRID:AB_2230769
Anti-mouse/rat CD62P	BioLegend	Cat# 148307 RRID:AB_2564110
Anti-mouse CD41	BD Bioscience	Cat# 553847 RRID:AB_395084
Anti-mouse IgG2a	BioLegend	Cat# 400263 RRID:AB_11149166
Bacterial and virus strains		
Escherichia coli (O111)	ATCC	Cat# BAA-2440
Chemicals, peptides, and recombinant proteins		
LPS from *E. coli*, Serotype O55:B5 (TLRGRADE™)	Enzo Lifesciences	Cat# ALX-581-013-L002
DAPI	Invitrogen	Cat# D1306
GSK484 (PAD4 inhibitor)	Cayman Chemical	Cat# 17488
FK506	Invivogen	Cat# tlrl-fk5
Cyclosporin A	Enzo Life Sciences	Cat# BML-A195-0100
MyrVIVIT - MAGPHPVIVITGPHEE	GenScript	Custom made
MyrVEET - MAGPPHIVEETGPHVI	GenScript	Custom made
PAR4-AP	MedChemExpress	Cat# HY-P1309
TRAP-6	Bachem	Cat# H2936
ARC-66096	Tocris	Cat# 3321
α-thrombin	Haematologic Technologies Inc.	Cat# HCT-0020
ϒ-thrombin	Haematologic Technologies Inc.	Cat# HCGT-0021
Collagen	Chrono-Log	Cat# P/N 385

(*Continued on next page*)

Continued

REAGENT or RESOURCE	SOURCE	IDENTIFIER
Epinephrine	Sigma-Aldrich	Cat# E4375
CountBright™ Absolute Counting Beads	Invitrogen	Cat# C36950
Apyrase	Sigma-Aldrich	Cat# A6410
PGE_1	Sigma-Aldrich	Cat# P5515
Fibrinogen	Sigma-Aldrich	Cat# F3879
Syto Green	Invitrogen	Cat# S7575
Sytox Orange	Invitrogen	Cat# S11368
Phosphatase inhibitors	A. G. Scientific	Cat# T-2494
FACS Lysing Solution	BD Biosciences	Cat# 349202
Intracellular Staining Permeabilization Wash buffer	BioLegend	Cat# 421002
Critical commercial assays		
IL-6 ELISA kit	BioLegend	Cat# 431301
Fibrinogen ELISA kit	Abcam	Cat# ab108844
Thrombin-Antithrombin complex ELISA kit	Abcam	Cat# ab137994
SuperSep Phos-Tag gel	Wako Pure Chemical Corporation	Cat# 198-17981
Experimental models: Organisms/strains		
Mouse C57BL/6J	Jackson Laboratory	Cat# 000664
Mouse B6Pin.C3-Ap3b1pe/J	Jackson Laboratory	Cat# 003215
Mouse Pf4-iCre	Jackson Laboratory	Cat# 008535
Mouse iNFATuation	GenOway	n/a
Software and algorithms		
GraphPad Prism 8.0.2	GraphPad	Prism - GraphPad RRID:SCR_002798
FlowJo software	Tree star	FlowJo v10.8 RRID:SCR_008520
ImageJ	NIH	ImageJ (nih.gov) RRID:SCR_003070
Amnis Ideas Software	Luminex Corporation	IDEAS 6.2

RESOURCE AVAILABILITY

Lead contact

Further information and requests for resources and reagents should be directed to and will be fulfilled by the lead contact, Ivan Zanoni (ivan.zanoni@childrens.harvard.edu; @Lo_Zanzi)

Materials Availability

The iNFATuation mouse strain will be made available upon request.

Data and Code Availability

- All data reported in this paper will be shared by the lead contact upon request.
- This paper does not report original code.
- Any additional information required to reanalyze the data reported in this paper is available from the lead contact upon request.

EXPERIMENTAL MODEL AND SUBJECT DETAILS

Mouse strains

6–8 week-old female and male wild-type (C57BL/6J, Jax 000664), Pf4-iCRE (Jax 008535), and *pearl* mice (B6Pin.C3-Ap3b1pe/J, Jax 003215), mutated in *Ap3b1* gene, were purchased from The Jackson Laboratory. *Pearl* mice are an established mouse model for Hermansky-Pudlack syndrome (HPS), thereby here referred to as HPS mice. $Nfat1^{-/-}$ mice were kindly provided by Dr. A. Rao. iNFATuation mice were generated by GenOway using the FLEx approach (Schnütgen et al., 2003). Briefly, this method is based on the Cre-lox system and uses two different *lox* sites, *loxP* and *lox2272*, that can only recombine with sites of the same type. When the lox sites are in opposing orientations, the Cre-recombinase inverts the DNA sequence between the sites. If the lox sites have the same orientation, the Cre-recombinase excises the DNA sequence between the sites. Mice were housed in pathogen-free conditions at Boston Children's Hospital, and all the procedures were approved under the Institutional Animal Care and Use Committee (IACUC)

and operated under the supervision of the department of Animal Resources at Children's Hospital (ARCH). SABV analysis has not been performed in this work.

Human participants

Human blood was obtained from healthy adult volunteers (males or females, >21 years old), who have not taken medication within a week before donation, or Hermansky-Pudlack syndrome patients (2 females, 2 or 3 years old; 1 male, 2 years old) or one Glanzmann thrombasthenia patient (male, 7 months old). Human study was approved by the Boston Children's Hospital Institutional Review Board, and all the participants provided written informed consent.

METHODS DETAIL

Murine platelets isolation

Murine blood was obtained from retro orbital plexus of wild-type (WT) or *Nfat1*$^{-/-}$ mice in sodium citrate as anticoagulant. For *in vivo* treatment with FK506 mice were injected daily with 4 mg/kg of FK506 for 14 days. Platelet-rich plasma (PRP) was obtained from whole blood by centrifugation at 100 × *g* for 10 minutes without brake at room temperature. Washed platelets were obtained by washing PRP with an equal volume of Tyrode's buffer with 0.02 U/ml apyrase and 140 nM PGE_1 at 2000 × *g* for 10 minutes. Platelet purity and count were assessed by flow cytometry. Platelet concentration was calculated using CountBright Absolute Cell Counting Beads (Thermo Scientific) according to the manufacturer's instructions.

Human platelet isolation

PRP was obtained from human blood by centrifugation at 110 × *g* for 12 minutes without brake at room temperature. Where indicated PRP was treated *in vitro* with indicated doses of FK506 or CsA prior to stimulation. Platelet purity and count were assessed by flow cytometry. Sample size can be found in figure legend.

Immunoblotting

20 × 10^6 washed platelets were stimulated for the indicated time points at room temperature and then were lysed using 5X western blot loading buffer. Immunoblotting was then performed with standard molecular biology techniques using 10% SDS-PAGE or pre-cast 7.5% SuperSep Phos-Tag gels (Wako Pure Chemical Corporation).

Platelet aggregation and secretion

PRP was stimulated in a Model 700 Aggregometer (Chrono-Log) with the indicated stimuli. Prior stimulation, luciferin-luciferase Chrono-Lume was added to measure secretion of dense granules content during aggregation recording. Aggregation curves and luminescence were recorded for 5 minutes. At the end of the test, ATP at known concentration was added to quantify the amount of ATP released.

Platelet activation markers assay by flow cytometry

PRP was stimulated with indicated stimuli in low-binding Eppendorf tubes. Simultaneously, samples were stained with antibody mix containing antibody for CD62P, active form of integrin αIIbβ3 and CD41 or CD42b for murine and human experiments respectively. After 15 minutes, samples were fixed with 1% formaldehyde in Tyrode's buffer. Data were acquired using a BD FACS Fortessa and analyzed with FlowJo software.

Platelet spreading assay

Glass coverslips were coated with fibrinogen (150 μg/ml) overnight at 4°C in a 24 multi-well plate. 2 × 10^6 washed platelets were seeded and stimulated or not with the indicated stimuli for 45 minutes at room temperature. Samples were fixed with 4% paraformaldehyde and permeabilized 10 minutes with 0.2% BSA 0.5% Triton X-100 in PBS. Then, samples were kept in blocking solution (2% BSA in PBS) for 30 minutes and actin was stained with phalloidin AlexaFluo488 (LifeTechnologies) in blocking solution for 20 minutes. Samples were mounted with ProLong (Invitrogen) and were imaged using a fluorescence wide-field microscope. Images were analyzed with ImageJ software (NIH).

Tail bleeding time

Mice were sedated with a mix of ketamine (100 mg/ml) and xylazine (20 mg/ml) and the tail was cut 4 mm from the distal tip. Blood drops from the tail were collected on blotting paper every 20 seconds until the complete stop of the bleeding. The bleeding time was defined as the time point at which there was no visible sign of blood on the blotting paper. For HPS mice, bleeding was manually stopped after 900 seconds due to their defect in coagulation.

Thromboembolism model

Mice sedated with a mix of ketamine and xylazine were injected with a combination of collagen (500 μg/kg, Chrono-Log) and epinephrine (3 μg/kg, Sigma). 60 minutes after injection, mice were observed and scored for a pathology index as following

described: 6 = dead, 5 = asleep without paw reflex, 4 = asleep with paw reflex, 3 = awake without paw reflex, 2 = awake with paw reflex, 1 = moving without paw reflex, 0 = moving with paw reflex.

Investigation of platelet-neutrophil complex formation by flow cytometry

Whole blood from WT or mice treated with FK506 was diluted 1:2 in Tyrode's buffer, stimulated with PAR4-AP for 30 minutes at room temperature and simultaneously stained with antibody anti-CD41, anti-Ly6G and anti-CD11b. Samples were then fixed with FACS Lysing Solution (BD Bioscience). Data were acquired using a BD FACS Fortessa and analyzed with FlowJo software.

Investigation of platelet-neutrophil complex formation by imaging cytometry

PRP was pretreated or not with 1 μM FK506 *in vitro* for 1 hour and then stained with antibody anti-CD9-PE or anti-CD9-APC, respectively for platelets that were not treated or FK506-treated. Platelets from these two different treatments were washed and mixed to be added to whole blood from platelet-depleted mice. Blood thus prepared was then stimulated or not with 25 μM PAR4-A and concomitantly stained for Ly6G. Samples were fixed with FACS Lysing Solution (BD Bioscience), washed, and resuspended in PBS with DAPI (0.2 μg/ml). Data were acquired with Amnis ImageStream Mk II (Luminex Corporation) and analyzed with Amnis Ideas Software. Platelet numbers were calculated with Spot Count Feature as PE or APC signal within the neutrophils $Ly6G^+$ mask.

In vitro platelets-induced NET formation

Murine neutrophils were purified from bone marrow of WT mice over a 62.5% Percoll gradient (GE Healthcare) as previously described (Mócsai et al., 2000). Neutrophils were seeded on fibrinogen-coated coverslip and stimulated 1 hour at 37°C with PRP previously stimulated or not with 150 μM PAR agonist for 5 minutes and pretreated or not for 10 minutes with 500 ng/ml of anti-P-selectin antibody or respective isotype control. Samples were fixed with an equal volume of 4% paraformaldehyde and then blocked with 2% BSA in PBS. Neutrophil extracellular traps (NETs) were stained with anti-citrullinate histone H3 (Abcam ab5103) overnight at 4°C, followed by anti-rabbit Alexa 568 secondary antibody. Nuclei were stained with DAPI. Samples were mounted with ProLong (Invitrogen) and were imaged using a fluorescence wide-field microscope. Images were analyzed using ImageJ software (NIH) and neutrophils were counted positive for NET formation when citrullinated histone H3 signal colocalized with DAPI staining.

LPS-induced septic shock

8-weeks old female mice were injected intra peritoneally with two doses of lipopolysaccharide (LPS O55:B5 serotype, Enzo Life Sciences), -4h 1 mg/kg and 0h 2 mg/kg. 2h after LPS challenge blood and peritoneal lavage were collected. Body temperature was measured every two hours with a rectal probe. Platelet and neutrophil counts were assessed in whole blood using CountBright Absolute Cell Counting Beads (Thermo Scientific) according to manufacturer's instruction. Plasma IL-6, fibrinogen and thrombin-antithrombin complexes were measured by ELISA. Peritoneal lavage was performed with PBS, cells were collected and stained for Ly6G, CD11b, CD41, and citrullinated histone H3. A secondary antibody anti-rabbit-Alexa 647 was used to detect citrullinated histone H3.

Gram-negative bacteria-induced sepsis

8-weeks old female mice were injected intra peritoneally with 1×10^8 CFU/mouse of *E. coli* (O111). 6 hours later, blood and peritoneal lavage were collected. Samples were processed as previously described for LPS-induced septic shock.

Platelet reconstitution model

Platelet depletion was induced in 10-12 weeks old WT mice by retro-orbital injection of anti-CD41 antibody (clone MWReg30, BioLegend), 250 μg/kg 2 days before platelet reconstitution and 100 μg/kg 1 day before platelet reconstitution. Peripheral platelet count to verify the depletion was determined by flow cytometry 18 hours after the second injection. For reconstitution, washed platelets from several donor mice were pooled and 10^9 platelets, treated or not with FK506, $Nfat1^{-/-}$ platelets were transferred intra-venously into platelet-depleted mice via retro-orbital injection. 30 minutes after platelet transfer, mice were subsequently subjected to sepsis induction.

Ex vivo NETs imaging

Mice were intra peritoneally injected with 1×10^8 CFU/mouse of *E. coli* (O111). 6 hours later, NETs formation was assessed in the peritoneal lavage and on the serosal surface of the peritoneal tissue, as previously described In vivo NETs imaging (Yost et al., 2016). Briefly, mice were sacrificed in a CO_2 chamber and the peritoneal fluid and membrane samples were harvested. The peritoneal cavity was rinsed with sterile PBS solution (200 μl per side) and analyzed for *in vivo* NET formation. Peritoneal fluids and membranes were placed on poly-L-lysine coated coverslip and stained for intracellular and extracellular DNA, with Syto Green and Sitox Orange (Invitrogen) respectively. NETs were analyzed using a Zeiss Axiovert 200M inverted confocal microscope (20X objective) and were quantified as number of intersections between the extracellular DNA signal and a standardized grid of 5 randomly selected fields of views per sample using ImageJ software (NIH).

QUANTIFICATION AND STATISTICAL ANALYSIS

Data were analyzed with GraphPad Prism statistical software (version 8). All data are presented as the mean ± SEM. For parametric data, statistical significance was analyzed using Student's *t*-test or ANOVA, as indicated in figure legends. Sample sizes for each experimental condition are provided in the figures and the respective legends. Asterisks were used as follows: *P < 0.05, **P < 0.01, ***P < 0,001 and ****P < 0,0001.